

Final Response

Dear Editor and Referees,

We are very grateful for the reviews and comments you provided on our paper entitled “Single-block rockfall dynamics inferred from seismic signal analysis.” Below we respond to the comments and suggestions provided.

We include the response made to the major points discussed by Referee 1 as in this letter we refer to answers we provided on several of the issues he raised.

The answer to a comment is given after repeating the comment and colored in **blue**. When changes have been made in the manuscript to take into account a suggestion we indicate the corresponding lines and page in the marked-up manuscript. The marked-up manuscript version showing the changes made is provided after our responses.

We hope that the revised manuscript is now suitable for a publication in *E-Surf*.

The authors.

JM Turowski (Editor) :

Dear authors, We have now received two reviews, and, since the discussion closes in a few days, I give a short summary of what I find important. While both reviewers are generally supportive of the manuscript, they both raise some criticisms that need to be addressed before publication. I add some comments of my own reading to that.

Presentation and language Reviewer #2 criticizes presentation and language and asks for rewriting with a focus on clarity. I agree that there are fairly frequent odd formulations and unclear writing.

We tried to improve the clarity and the overall language in the whole manuscript.

Scaling, linearity and the fits Reviewer #1 raises concerns about the terminology used in the paper. I do not agree with his definitions; in my understanding, two variables A and B scale with each other, if they have a positive monotonic relationship, without the need of specifying a function. That is, if A increases, B increases also. Two variables are proportional if their ratio is a constant. And they are linearly related if $A=mB+b$, where m and b are constants. However, I agree with reviewer #1 that in the manuscript, the terminology is not used in a common way. For example, I would not say that two variables scale linearly, but rather that they have a linear relationship of linear dependence. That said, there is something funny about the plots in Fig. 4 and the way the relationships are discussed. The plots in Fig. 4 are all log-log. In this representation, proportionality would result in a straight line with a gradient of one. A linear relationship would result in a curved line. A closer look reveals that the depicted fit lines actually have gradients that deviate from one. They show power law relationships. The fit values given in Table 2 indicate exponents of up to 2. This may change the entire results, discussion and outcomes of the paper. Here is at least a major problem with the communication, if not with the use of the fits and the statistical relationships. These need to be carefully resolved and communicated.

Following this remarks and the suggestions of Referee 1 we reorganized the paper and changed significantly the results section of the paper (p.8-p.11). We clarified our approach and the terminology used as suggested.

Regarding the power-law assumption : There are indeed α coefficients close to 2 when looking at the regression laws found in the log-log space, but those coefficients are obtained for pair of parameters that we think are not strongly correlated (“Seismic energy” and “mass” for example). Moreover, the uncertainty of those coefficients is large. For example, with the pair of parameters “seismic energy” and “kinetic energy”, $\alpha=1.38$ but with 95% coefficients bounds of +/- 0.4. Moreover, all the other studies (e.g. Deparis et al., 2008; Hibert et al., 2011, 2017; Yamada et al., 2012; Levy et al., 2015) that sought correlations between the seismic features and the event properties found linear relationships. Therefore we decided to remove the results obtained in the log-log space and we included a short-paragraph in the “results” section to explain why we choose to fit the data with linear relationships (p.10 l.26-29).

Relation to theory Reviewer #1 comments that the relations to his theory are partially incorrect and not well described. In light of the issue raised in the preceding point, I ask the authors to clearly present the used theory in the paper, identify appropriate hypotheses that can be tested with the data (both a theory-derived hypothesis and a null hypothesis), and to discuss how the outcomes of their experiments relate to these.

We agree and added a paragraph (p.8 l.13-18 and p.10 l.1-8) explaining the assumptions tested.

Energy budget I also like reviewer #1’s suggestion of the energy budget and ask the authors to provide appropriate calculations and a discussion on this.

We agree and added a paragraph in the discussion (p.13 l.20-32) (also see response to Referee 1 comment).

Relationship between seismic energy and amplitude The authors should also investigate and discuss the relationship between seismic amplitude and energy and how this would impact their analysis.

We computed a correlation coefficient between these two parameters (see comment below) and included it in Table 1 to show that they are not correlated. (Also see response to the comment of Referee 1 on this issue).

Significance and fit values. The authors argue the significance of their trends based on C2 goodness of fit statistics such as R2. There are at least a few instance (especially when claiming no significant relation), where a non-parametric statistic such as Kendall’s tau would be more appropriate.

We agree and we modified the “result section” accordingly. We chose the Spearman’s rho non-parametric statistic measure as we assume that our data should scale following a monotonic law. (p.10 l.7-21)

Please note that all reviewers’ comments that I have not mentioned should also be treated with due care.

2.30 These authors. . .

3.15 French Alps (French with capital letter)

5.3 . . .dependent on. . .

9.19 . . .for blocks for which. . .

9.25 . . .the uncertainties associated with determining the amplitude at the source are lower than those associated with seismic energy.

Referee 1 :**Review by M. Farin****General comments :**

The paper is globally clear to read and the successive sections follow naturally each others. I find personally that it is interesting to have new data of seismic signals generated by block impacts and be able to evaluate the dynamics of the block in parallel in order to better understand the link between the two on the field. The authors took care to evaluate the dynamics of the block with a good precision, with an uncertainty less than 1 m s^{-1} for block speeds varying from 6 m s^{-1} to 17 m s^{-1} . When we compare seismic parameters to dynamic parameters, it is important to evaluate the absolute seismic parameters at the source because they strongly depend on the distance between the source and the instrument and on the frequency. Care has also been taken in evaluating absolute seismic parameters in this paper. Therefore I think the presented data are of good quality. However, I think that the paper needs a major revision before being considered for publication because it contains major confusions and misinterpretations of the data.

- My main concern is the fact that the authors say several times in the paper that they show a scaling (or proportionality) between the seismic amplitude and the momentum of the block while they are showing a linear relationship. There is a important confusion here because a scaling (or proportionality) is a relation $Y = a X$ while a linear relationship (as showed in this paper) is $Y = aX+b$, with b a nonzero constant. This has a different implication for the interpretation of the data. The paper should be rewritten with this point in mind. This confusion is particularly problematic when the authors are comparing the parameter $mVz^{13/5}$ derived by Farin et al. (2015) to the radiated seismic energy E_s . They are testing a law $E_s = a mVz^{13/5} + b$ and claim that the fit of this law with their data is better than it was in the paper of Farin et al. (2015). However, the analytical scaling law established in Farin et al. (2015) and tested with their rockfall experiments was $E_s = a mVz^{13/5}$ (with $b=0$): this is a different law. In the present paper, the parameter b is not 0 and it is several orders of magnitude larger than the parameter a . The fit $E_s = a mVz^{13/5}$ (with $b=0$) should be tested instead. Moreover, since the parameter b does not exist in the analytical model, I do not know if this parameter has a physical meaning, even though it has the dimension of an energy. Also, an analytical expression of the proportionality coefficient a is given in Farin et al. (2015). The exact law and empirical law (with the exact and empirical value of a) could be compared to the seismic energy E_s .

Our first intention was to process the data for single rockfalls and seek for the best relationships as it was done in other studies on large landslides or rockfalls (e.g. *Deparis et al., 2008, Hibert et al., 2017*). In those studies, the best correlations were found using linear relationships, which naturally led us to use the same approach for this study. We agree, in the light of the comments made by the referees and the editor, that proportionality laws have to be tested too, and the confusion between linear and proportional relationships lifted.

To address this comment we computed proportional laws for each pair of quantities chosen. We modified table 2 to show these results. The new Table 2 is reproduced below and in the revised

version of the manuscript is relabelled as Table 1. For the sake of clarity, we also decided to remove the coefficients computed in the logarithm space, as we discuss and use only the relationships computed in the linear space in the rest of the paper. We will also modify figure 4 to show the data in the linear space, and add the regression lines associated with proportional relationships.

Table 1 : New table 1 : Spearman correlation coefficients, coefficients of the regression lines for proportional and linear relationships and corresponding coefficient of determination

Parameters (X, Y)	Spearman correlation		Proportional			linear		
	ρ	p -values	α	β	R^2	α	β	R^2
$A0_{max} = \alpha p + \beta$	0.67	$1.12 \cdot 10^{-7}$	$2.35 \cdot 10^{-9}$	0	0.63	$2.26 \cdot 10^{-9}$	$2.50 \cdot 10^{-7}$	0.64
$E_s = \alpha E_p + \beta$	0.68	$6.75 \cdot 10^{-6}$	$4.40 \cdot 10^{-6}$	0	0.61	$5.04 \cdot 10^{-6}$	-0.01	0.61
$E_s = \alpha E_k + \beta$	0.70	$3.01 \cdot 10^{-6}$	$2.59 \cdot 10^{-6}$	0	0.59	$3.09 \cdot 10^{-6}$	-0.01	0.64
$E_s = \alpha m + \beta$	0.51	$1.3 \cdot 10^{-3}$	$1.48 \cdot 10^{-4}$	0	0.23	$2.85 \cdot 10^{-4}$	-0.03	0.31
$E_s = \alpha m V_z^{13/5} + \beta$	0.69	$4.16 \cdot 10^{-6}$	$4.86 \cdot 10^{-7}$	0	0.62	$5.85 \cdot 10^{-7}$	-0.01	0.63
$E_s = \alpha m V_z^{0.5} + \beta$	0.62	$7.63 \cdot 10^{-5}$	$5.24 \cdot 10^{-5}$	0	0.33	$1.07 \cdot 10^{-4}$	-0.04	0.47
$A0_{max} = \alpha E_s + \beta$	0.44	$8.2 \cdot 10^{-3}$	-	-	-	-	-	-

As shown by this new table, the regression of our data by proportional laws yields slightly worst fits (lower R^2 values), but with α coefficients very close to the one returned by linear regression. The coefficients β in the linear regressions are close to zero (even if order of magnitude larger than coefficients α). This might explain why the coefficient α and R^2 returned by the proportional relationships are very close to the one observed for the linear ones. The slightly better fit achieved by linear regressions might come from the accommodation of the uncertainties on the values of the tested parameters, which are inherent to the processing of real data. We added a comment on this point in the revised manuscript (p.11 l.4-6).

The paper will be modified by taking into account these new results, however this will not impact the main conclusions of our work, which are: (i) Linear/proportional relationships exist between the maximum amplitude and the momentum, and between the seismic, the kinetic and the potential energies, and (ii) we can retrieve rockfalls properties directly from the seismic signals generated at impacts.

- An interesting question when we study the seismic signal generated by rockfall is to establish their energy budget, i.e. determine the amount of kinetic energy or potential energy lost that is radiated in the form of elastic waves. In other words, I think the authors should compute the value of the ratios E_s/E_k and E_s/E_p (or maybe also $E_s/(E_k+E_p)$). These ratios should be less than 1 and the rest of the kinetic and/or potential energy lost is dissipated in plastic deformation (irreversible deformation) of the ground or in viscoelastic processes (heat). These ratios can then be compared with that computed for larger rockfalls in the crater of the Piton de la Fournaise, La Reunion Island (Hibert et al. 2012) or with that obtained in other studies (e.g. Deparis et al. 2008). Thus we could see if the energy budget for one single impactor is different than for a rockfall constituted of several blocks. These ratios are proportionality relations between seismic and dynamic parameters.

Those ratios are directly given by the relationships we found (see table above). We will add a comment in the discussion on these values, which are slightly lower than the one computed at Piton de la Fournaise or Soufrière Hills volcano (10^{-6} vs. $10^{-5} - 10^{-3}$). We suspect that the nature of the substrate (black-marls, i.e. soft sediments) can be the cause of these lower ratios (p.13 l.20-32).

- In a nutshell, I think that proportionality relationships $Y=aX$ between seismic and dynamic parameters would have much more interesting implications for interpretations of the seismic signals generated by rockfalls than linear relationships $Y=aX+b$. Besides, no confusion should be made between the two kinds of relationship. A linear relationship may better fit the data of this paper than

a proportionality law $X = a Y$ but in this case, both fits ($X = aY+b$ and $X = aY$) should be shown and a physical interpretation of parameter b should be given.

(see comment above).

- An other problem I see is when the authors want to retrieve the mass and the speed of the blocks from the seismic signal. Two seismic variables are used: the absolute seismic amplitude and the radiated seismic energy. However, I do not think these two variables are independent of each others. I would not be surprised if the radiated seismic energy is proportional to the squared absolute amplitude. In this case, the mass and the speed could be expressed as functions of the radiated seismic energy alone. The problem is that I don't think it is possible to retrieve two independent dynamic parameters from only one seismic variable.

We do not correlate the absolute seismic amplitude to the momentum but to the *maximum* of the amplitude envelope. This is an important distinction as the *peak* amplitude might not be correlated to the seismic energy (integral of the envelope). For example, a long –duration seismic signal with no clear peak amplitude might have the same seismic energy as an impulsive, high–amplitude, short–duration seismic signal. As shown by the computed Spearman's correlation coefficient (Table) and the figure below with our data, these quantities are not dependant in our case.

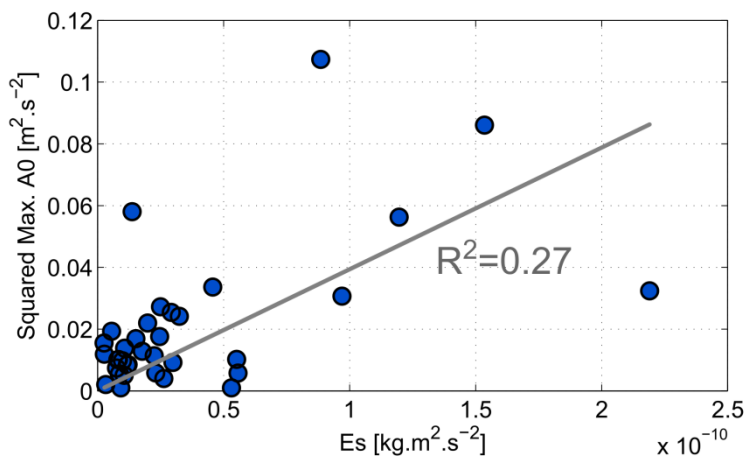


Figure 1: Squared maximum amplitude A0 as a function of the energy of the seismic signal generated at each impact

An advantage of the present study compared with the previous ones (e.g. Farin et al. (2015)) is that the authors have access to higher frequencies up to 500 Hz, with respect to 50 Hz before. Therefore, they potentially have access to all the frequencies emitted during the impacts, contrary to the previous study. Thus an interesting seismic parameter to evaluate would be the mean frequency of the seismic signal. the analytical model of impact of Hertz shows that the mean frequency is inversely proportional to the mass m of the block. It would be interesting to test this scaling. The mean frequency of the signal is independent of the radiated seismic energy so if empirical scaling laws are established between these two parameters and the mass and the speed of the block, the laws can be inverted to retrieve the masses and the speeds. Farin et al. (2015) established two analytical scaling laws relating the mass and the speed of the block to the radiated seismic energy and the mean frequency of the signal, i.e. equations (29) and (30) of their paper. I would be curious to see if these equations can provide reasonable values of the masses m and the speeds Vz of the blocks with the present experiments.

Regarding an approach based on the frequency content, there are two limitations. The first one is that the seismometer located down-slope has a Nyquist frequency of 50 Hz. Hence, we had to restrict our study to the 1-50 Hz frequency band, as most of the times we need this station to compute the attenuation parameters and thus the amplitude and the energy at the source. Second,

because we are lacking a good propagation model, we cannot reconstruct the Green's function of the medium between the location of each impact and the stations. Without these Green's functions, it is impossible to extract the frequency content of the source. This prevents any analysis of the frequency content of the seismic signal of each impact, as we cannot decipher the source effects from the propagation effects. As clearly shown by Figure 2b, the major control on the frequency content of the seismic signal recorded at each impact is related to its distance to the station. Therefore it makes no sense to compute the average frequency, as it is predominantly controlled by the medium and not the source.

This underlies that an implementation of a frequency-based approach for the quantification of rockfall properties from the seismic signal they generate would be difficult in an operational context. The new approach we propose in this study does not require a thorough characterization of the medium, and we show that we can determine rockfalls properties simply from the seismic signal temporal features.

- Maybe the absolute seismic amplitude and the radiated seismic energy are independent of each others. In that case it should be shown somewhere. Besides, if the mean frequency of the signal is not inversely proportional to the mass of the block, it would be interesting to show it. That would mean that Hertz's model does not apply on the field.

(See comment above)

Comments on specific lines in the paper:

- The abstract needs a context sentence.

We added a context sentence (p.1 l.2-3)

- page 1 line 8, line 10..., ' the energy of the corresponding part of the seismic signal ', 'the energy of the seismic radiation',... try to always call this energy is the same way all along the paper, for example 'the radiated seismic energy' because it is sometimes difficult to understand to what energy you are referring to.

We agree and made the proposed modification.

- page 1 line 8: 'Our results suggest that the amplitude of the seismic signal scales with the momentum of the block at the impact.'. No, be careful thorough in the paper: a scaling is a proportionality, not a linear relationship. This is important.

Revised.

- page 1, line 12: ' the masses and the velocities ' or ' the mass and the velocity '

Revised

- page 2, line 19: precise that this is true in the frequency range 3 Hz to 10 Hz

Precision added.

- page 2, line 20: 'The authors also demonstrated that the maximum amplitude of the seismic signal, corrected from propagation effects, scales with the bulk momentum': That was also a linear relationship, not a scaling (i.e. proportionality).

Revised

- page 2, lines 27-32: this paragraph needs rewriting: line 30: 'The impulse imparted to the solid Earth by a bouncing particle within a granular flow will be proportional to the kinematics of the particle, and the amplitude of the seismic wave will be proportional to the magnitude of the impulse'. This sentence is not very clear, it particular 'proportional to the kinematics of the particle' does not mean anything:

This suggests that we do not know yet which kinematic parameters control the impulse that generates the seismic waves. It could be the velocity, but also the momentum, the kinetic energy, etc. We modified slightly this sentence to make this point clearer. (p.3 l.4)

- page 2, l. 34: not exactly true: the mass and the speed of an impactor can be related to the radiated elastic energy and the mean frequency of the signal. Do not write 'at a given frequency', it could be misinterpreted.

Agreed and revised.

- page 3, l.1: precise here what is the relation you are referring to: $E_s = a mv^{13/5}$.

Here we are not only referring to this relation but to the several tested in Farin et al., (2015). This relation, as well as others, is discussed later in the paper and we do not think this equation needs to be already explicitly mentioned in the introduction.

- page 3, l.4: It is very strange for me why you say that having frequency < 50 Hz is a limitation (which is true) but then you are filtering your signals below 50 Hz in the following (p 6, l 30). Why don't you take advantage of having frequencies higher than 50 Hz in order to improve the estimate of the masses and speeds of the blocks with respect to the previous study? Moreover, you know the mass and the speed of the blocks so you can evaluate a theoretical mean frequency of the signal generated by an impact using Hertz theory of impact and then compare with the measured mean frequency in your data. You would know if your seismic stations are sensitive to the whole frequency spectrum emitted during the impact or if you are losing energy in the highest frequency (if the measured mean frequency is smaller than the theoretical mean frequency). This would help you to interpret the difference between the measured radiated seismic energy E_s and the parameter $a mv^{13/5}$: normally the measured E_s should be smaller than $a mv^{13/5}$ at high frequency if you are not sensitive to the highest frequencies. Finally, if you don't obtain any satisfying results using the mean frequency, it would mean that the mean frequency is not a reliable enough parameter to use to extract information from the seismic signal generated by impacts on the field: this is an interesting result.

(See general comments above)

- page 3, l. 4, you should rather say 'a great part of the energy liberated at the impact is at high frequencies (> 50 Hz) ...'. Another important limitation we had was that there was no synchronization between the seismic signal and the movies...

We rewrote this sentence. (p.3 l.14-16)

- page 3, l.6-11: You should better highlight what is new in your study with respect to the previous study: you use several seismic stations that can record higher frequencies, up to 500 Hz and a better identification of the seismic signals associated with each impact of the blocks.

We completed this sentence as suggested.

- page 3, l.25: Is the torrent producing a lot of seismic noise?

No, the torrent was almost dry at the time of the experiment.

- page 4, l.6: Define clearly what are the potential energy lost and the kinetic energy as a function of the mass and the speed of the block, and show these relations on the axis of Figure 4. Also: is the speed of impact V_z vertical or inclined with respect to the slope/vertical? Can you observe an effect of the angle of impact with respect to the normal to the slope on the radiated seismic energy? Are more inclined impacts less seismically efficient (lower E_s/E_p) than more normal impacts? This might potentially explain part of the discrepancy.

V_z is the vertical velocity. We added the equations used to compute the kinetic and the potential energies (Eq. 1 and Eq. 2). We do not think showing these equations on the axes of figure 4 is useful.

We do not observe an effect of the angle of impact on the energies ratio but this might not be significative as the uncertainties on the computation of the seismic energy are large.

- page 4, l. 11: Write here the range of values the speed of impacts V_z can take because we don't know if 1 m s^{-1} is a large and small uncertainty.

Precision added.

- Figure 1c: not clear what the colored points are referring to. The text in the figure is too small, especially along the torrent.

Precision added in the caption. We increased the font size of the text.

- page 5, l. 4, the Figure 2b also shows the attenuation of small frequencies. Rephrase the sentence.

We do not understand this comment. Figure 2b predominantly shows the attenuation of high frequency waves. Lower frequencies are visible at each impact, hence this figure does not illustrate any attenuation of the low-frequency seismic waves.

- page 5: It is not clear how you obtain the equation (2) and what the index ij are representing for B . You should directly say that B depends on frequency and show B as a function of the frequency, on a Figure for example (maybe in Appendix), so that we can know what is the quality factor Q . If you assume that B does not vary with frequency then give the value of B (or a range of values).

B_{ij} is the average values of the anelastic attenuation coefficient B for an impact recorded on station i and station j , as explained on lines 5-7 p6. We do not think giving the corresponding value of Q is relevant, as B is an *apparent* anelastic attenuation parameter, which may not reflect the true attenuation coefficient of the medium.

- page 5, l. 23: Can you measure the wave speed in this specific site with your present seismic data by measuring the difference of time travel after an impact between several seismic stations?

This should be possible but would require significant processing and is not the main focus of this paper.

- page 6, l. 30: What a pity not to use the high frequencies $> 50 \text{ Hz}$. There may a lot of interesting information in it.

(see general comment)

- Figure 4:

- Do you observe a correlation between radiated seismic energy E_s and the squared momentum $|p|^2$?

(see general comment)

- See my first comment about the law $X = a Y$ and the energy ratios.

(see general comment)

- See my first comment: the laws established and tested in Farin et al. (2015) are $E_s = a mV_z^{13/5}$ and $E_s = a mV_z^{0.5}$, not the ones you are showing.

(see general comment)

- The caption of the figure can be simplified: 'Decimal logarithm of the seismic energy E_s of the seismic signal generated at the impact as a function of (b) E_k , (c) Mass, (d) E_p , (e) $mV_z^{0.5}$ and (f) $mV_z^{13/5}$.'

Caption revised.

- page 9, l. 3-9: Rewrite this paragraph in accordance with my first comment.- page 9, eq. (6): I am not sure that the absolute amplitude and the radiated elastic energy are independent variables. Also write explicitly the equation for the speed V_i as a function of the signal parameters.

(see general comment)

We added the equation for the speed V_i (Eq. 8).

- Table 1, Fig 5: Represent the results of the inversion more uniformly: a figure with two plots showing (a) m_i as a function of m_r and (b) V_i as a function of V_r , with error bars and the line $Y=X$ would be much clearer than a table and a histogram that mean to represent the same thing for m and V_z .

We think that a table is more appropriate, as it includes the number of impacts used to compute the inferred mass. As commented in the text, the number of impacts used reduces the uncertainty on the determination of the mass. This is important to show. The histogram, is, in our opinion, easier to interpret for the readers.

- page 11, l.4: 'linear scaling' => linear relationships.

Revised.

- page 11, l. 7: 'the seismic radiation released at each impact scales linearly with the potential energy lost': no.

We meant here that the seismic energy radiated is correlated with the potential energy, which is true according to our result. We modify this sentence to make this point clear.

- page 11, paragraph 2:

- You did not verify this scaling law either.

(see general comment)

- 'In our study the instruments we deployed permitted to record most of the energy generated at impacts. This underlines the importance of choosing adequate seismometers, capable of recording the whole seismic energy generated at the impacts, for future studies.': Yes but you did not take advantage of this because you filtered the signals below 50 Hz while energy is clearly visible at more than 200 Hz on Figure 2a... Therefore you can not use this sentence to explain why you observed better correlations.

We agree and modified this paragraph.

- page 11, last line: ' We show that the maximum amplitude of the seismic signal generated by the impact of a single particle is proportional to its momentum. ' This is false.

According to our results, this is true.

- page 12, first line: 'The source of the seismic signal generated at this given time might therefore be the sum of the impulses imparted by the particles to the ground.' I do not think we can say that because the signals emitted by two particles impacting the ground at roughly the same position and time can destruct or add themselves, depending of their phase. The energies of each impacts may be added, however (see the paper of Tsai et al. 2012 on the seismic noise of river: ' A physical model for seismic noise generation from sediment transport in rivers ', GRL (2012).). Moreover, in the granular flow experiments we did with Anne Mangeney during my PhD (cf. Farin, M. (2015), Étude expérimentale de la dynamique et de l'émission sismique des instabilités gravitaires. IPGP, France.), we showed that the scaling law that relate the radiated seismic energy to the mass for a single impactor is not the same as for a granular flow of multiple particles of the same size. The relationship between the radiated seismic energy and the mass and the speed of the particles in a granular flows is much more complex than for one impact because all the particles are interacting with each others and each of them move in a random direction with respect to its neighbors (in an agitated flow) and each of them has a different fluctuating speed (instantaneous speed - mean speed of the flow). Therefore, the seismic amplitude generated by a granular flow does not simply scale (nor has a linear relationship) with the momentum of one particle in the flow. As you say in the last sentence, numerical models (DEM or statistical models like kinetic theories of granular gas) can help us better understand the complex link between particle/flow dynamics and seismic signal in granular flows.

We agree with those insightful remarks and moderated the last paragraph of the discussion.

Referee 2 :

Review by F. Panzera

The manuscript "Single-block rockfall dynamics inferred from seismic signal analysis" by Hibert et al. is interesting and contains innovative information about seismic radiation due to rockfall. Below some comments that I hope help the authors in improving the manuscript.

Although I am not an English mother-tongue, at times I found some sentences difficult to follow. In my opinion, the authors should improve the English language.

We tried to identify and improve the sentences that were difficult to understand.

In the Introduction, few lines should be added on the importance of rockfalls characterization, through seismic method (but not only). See for instance:

Burjanek J., Moore J.R., Yugsi-Molina F.X., Fah D. (2012) Instrumental evidence of normal mode rock slope vibration. *Geophys. J. Int.*, 188, 559–569.

F. Panzera, S. D'Amico, A. LotC1 teri, P. Galea, G. Lombardo (2012) Seismic site response of unstable steep slope using noise measurements: the case study of Xemxija bay area, Malta. *Nat. Hazard Earth Sci. Syst.*, 12, 3421–3431 doi: 10.5194/nhess-12-3421-2012

P. Galea, S. D'Amico, D. Farrugia (2014) Dynamic characteristics of an active coastal spreading area using ambient noise measurements – (Anchor Bay, Malta). *Geophys. J. Int.*, 199, 1166–1175 doi: 10.1093/gji/ggu318.

These studies are not focused on the relationships between the dynamics of rockfalls and the seismic signal they generate but more on the use of the seismology to monitor the state of instable slopes or cliffs. However we agree that this other use of the seismology to mitigate risks associated with mass movements should be mentioned in the introduction, and we included these references and others [Amitrano et al., 2005; Levy et al. 2011]. (p.2 l.1)

In Figure 1a and b, what do the authors indicate with blue points? Which is the meaning of coloured points in Figure 1c?

As stated in the caption the blue points on figure 1a and b are the ground control points. We added the information on the meaning of the coloured points corresponding to the trajectory in the caption.

In Figure 1c, I understand that CMG1 is the broadband seismometer, but it is unclear which is the 3D short-period seismometer between K1, K2, K3 and K4. The authors should add a legend in map or some description in the figure caption.

We completed the figure caption.

The authors assume that seismic wavefield, generated by rockfalls, is composed mainly by surficial waves and consequently that the contribution of body waves is negligible. They must support this hypothesis through observations or by quoting references.

We provided references (p.5 l.1-3)

The authors assume that seismic wave velocity in black-marls is 300 m/s quoting as references Hibert et al. (2012) and Gance et al. (2012). Are the quoted studies performed in the same formations near Rioux Bourdoux? The sentence must be rewrite as follow: “The average velocity of surface waves in black-marls in the area of Rioux Bourdoux is approximately 300 m/s (Hibert et al., 2012; Gance et al., 2012).” or “The average velocity of surface waves in black-marls, considering information coming from literature, is approximately 300 m/s (Hibert et al., 2012; Gance et al., 2012).”

Yes the studies to which we refer to were done in the same formation (black-marls). We modified the sentence as suggested.

I suppose that the propagation depth is obtained by considering $\lambda_{pda} = v/f$. This assumption should be quoted in the text and the authors must specify why they chosen 20 Hz as central frequency for their computation.

We added this clarification in the text (p.6 l.21)

The authors used a linear regression to interpolated their data. Did they try to use a C2 power or logarithm law using a lin-lin graph? The R² for each linear regression curve should be visible in the graphs of Figures 4.

We added the R² of each regression in Figure 4. Regarding other laws, see the response to the editor comment.

Probably in the case of x and y having uncertainties a Generalized Orthogonal Regression is need instead than standard least-squares.

Most of the studies we refer to in this manuscript used to quantify the good fit of their data with the standard least-squares estimator. For an easier comparison of our results with the ones already discussed in the literature we find it more convenient to use the same estimator.

The term “proportional” used in the manuscript is not correct, because the authors use a linear regression ($y=ax+b$) with a non-zero “b”.

(See response to the general comment of referee 1)

Single-block rockfall dynamics inferred from seismic signal analysis

Clément Hibert¹, Jean-Philippe Malet¹, Franck Bourrier², Floriane Provost¹, Frédéric Berger²,
Pierrick Bornemann¹, Pascal Tardif², and Eric Mermin²

¹Institut de Physique du Globe de Strasbourg - CNRS UMR 7516, University of Strasbourg/EOST, 5 rue Descartes, 67084
Strasbourg, France

²Institut national de recherche en sciences et technologies pour l'environnement et l'agriculture (IRSTEA), 2 Rue de la
Papeterie, 38402 Saint-Martin-d'Hères, France

Correspondence to: Clément Hibert (hibert@unistra.fr)

Abstract. ~~We~~

Seismic monitoring of mass movements can significantly help to mitigate the associated hazards, however the link between event dynamics and the seismic signals generated is not completely understood. To better understand these relationships, we
conducted controlled releases of single blocks within a soft-rock (black marls) gully of the ~~Rieux-Bourdoux~~ Rieux-Bourdoux
5 torrent (French Alps). 28 blocks, with masses ranging from 76 kg to 472 kg, were used for the experiment. An instrumentation
combining video cameras and seismometers was deployed along the traveled path. The video cameras allow ~~to reconstruct~~
reconstructing the trajectories of the blocks and ~~to estimate~~ estimating their velocities at the time of the different impacts with
the slope. These data are compared to the recorded seismic signals. As the distance between the falling block and the seismic
sensors at the time of each impact is known, we were able to determine the associated seismic signal amplitude corrected from
10 propagation and attenuation effects. We compared the velocity, the ~~loss of potential energy~~ potential energy lost, the kinetic
energy and the momentum of the block at each impact to the true amplitude and the ~~energy of the corresponding part of the~~
~~seismic signal~~ radiated seismic energy. Our results suggest that the amplitude of the seismic signal ~~scales with~~ is correlated
to the momentum of the block at the impact. We also found ~~a scaling law~~ relationships between the potential energy lost,
the kinetic energy and the ~~energy of the seismic radiation generated~~ seismic energy radiated by the impacts. ~~By combining~~
15 ~~these scaling laws, we inferred~~ Thanks to these relationships, we were able to retrieve the mass and the velocity before impact
of each block directly from the seismic signal. Despite high uncertainties, the values found are close to the true values of
the ~~mass~~ masses and the velocities of the blocks. These relationships also provide new insights to understand the source of
high-frequency seismic signals generated by rockfalls.

1 Introduction

20 Understanding the dynamics of rockfalls and other mass movements is critical to mitigate the associated hazards but is very dif-
ficult because of the limited number of observations of natural events. With the ~~increasing~~ densification of the global, regional
and local seismometer networks, seismic detection of gravitational movements is now possible. The continuous recording abil-
ity of seismic networks allows a reconstruction of the gravitational activity at unprecedented time scale and the monitoring of

unstable slopes (e.g. Amitrano et al., 2005; Helmstetter and Garambois, 2010; Levy et al., 2011; Burjáněk et al., 2012; Panzera et al., 2012)

More than the detection of these events, recent advances allow ~~to determine~~ determining the dynamics of the largest landslides on Earth from the very low-frequency seismic waves they generate. Inversion and modeling of the long-period seismic waves permits to infer the force imparted by these catastrophic events on Earth, and to deduce dynamic parameters (acceleration, velocity, trajectory) as well as their mass (Favreau et al., 2010; Schneider et al., 2010; Moretti et al., 2012; Ekström and Stark, 2013; Allstadt, 2013; Yamada et al., 2013; Hibert et al., 2014a, c). However, these approaches are limited by the size of the events. Only the largest landslides will generate the long-period seismic waves used in the inversion and the modeling methods. ~~These~~ Moreover these events constitute only a small proportion of the landslides that occur worldwide.

In recent years, a new approach based on the analysis of the high-frequency seismic signal has been proposed. High-frequency seismic waves are generated independently of the size of the event, and can be recorded ~~if~~ if seismometers are close enough to the source. Hence, this allows a seismic detection of the events that do not generate long-period seismic waves (e.g. Deparis et al., 2008; Helmstetter and Garambois, 2010; Dammeier et al., 2011, 2016; Hibert et al., 2011, 2014b; Clouard et al., 2013; Chen et al., 2013; Burtin et al., 2013; Tripolitsiotis et al., 2015; Zimmer and Sitar, 2015). The limitation of this approach is that high-frequency seismic waves are more prone to be influenced by propagation effects (attenuation, dispersion, scattering) and, more importantly, that the source of the high-frequency seismic waves associated with gravitational instabilities is not well understood yet.

~~Several studies~~ Studies have shown that ~~some~~ several landslide properties can be linked to features of the high-frequency seismic signals. In some cases, it has been ~~shown~~ observed that the landslide volumes ~~can be linked~~ is correlated to the amplitude (Norris, 1994; Dammeier et al., 2011) or to the radiated seismic energy of the high-frequency ~~seismic~~ signals (Hibert et al., 2011; Yamada et al., 2012). ~~Several~~ Other studies have shown that the high-frequency seismic signals can also carry information on ~~the~~ landslide dynamics. Schneider et al. (2010) have ~~shown, thanks to numerical modeling,~~ determined with numerical modeling that a good correlation exists between the short-period seismic-signal envelope, the modeled friction work rate and the momentum (product of the mass and the velocity) for two rock-ice avalanches. The model-based approach proposed by Levy et al. (2015) has shown that a correlation can be found between the modeled force and the power of the short-period seismic signal for rockfalls that occurred at the Soufrière Hills volcano on Montserrat Island. ~~? have shown~~ Hibert et al. (2017) have demonstrated that, for 11 large landslides that occurred worldwide, the bulk momentum controls at the first order the amplitude of the envelope of the generated seismic ~~signal. The~~ signals filtered between 3 Hz and 10 Hz. These authors also demonstrated that the maximum amplitude of the seismic signal, corrected from propagation effects, ~~seales~~ is quantitatively correlated with the bulk momentum. These results are important as they open the perspective to quantify the landslide dynamics, independently of their size, and directly from the seismic signals they generate (i.e. without inversion or modeling). Being capable of quantifying the landslide properties directly from ~~their seismic signals~~ the seismic signals they generate is critical for the development of future methods ~~for their~~ aimed at their real-time detection and characterization using high-frequency seismic ~~signal in real-time~~ signals. However, before considering an operational implementation of such methods, we need to better understand the source of the high-frequency seismic radiations ~~associated, and the observations~~ made on the link between these radiations and the generated and their links with the landslide dynamics.

One of the assumptions that ~~emerges~~ emerge from these studies to explain the link between the landslide dynamics and the high-frequency seismic signal features is that this relationship can potentially ~~reflects the sealing of~~ originate from small-scale processes within the landslide mass, and between the landslide mass and the substrate. The impulse imparted to the solid Earth by a bouncing particle within a granular flow ~~will~~ might be proportional to ~~the kinematics of the particle~~ its dynamics, and the amplitude of the seismic wave ~~will~~ might be proportional to the magnitude of the impulse. However, this assumption raises an important issue: what is the link between the dynamics of a single bouncing particle (a rock for example) and the seismic signal ~~it generates~~ generated?

Theoretical developments, laboratory and field experiments were conducted by Farin et al. (2015) to address this issue. ~~The~~ These authors have shown that the mass and the speed of an impactor can be related to the radiated elastic energy ~~at a given~~ frequency and to the spectrum of the signal, following analytic developments based on the Hertz theory of impact (Hertz, 1882). However, the field experiment conducted showed that, in this case, these simple ~~relations~~ relationships did not perform well to quantify the velocity and the mass of single rocks from the seismic signal it generates. ~~The major limitation they identified is that a great part of the energy liberated at the impact is lost in high frequencies (> 50 Hz), but the seismometer used during the field experiment~~ Difficulties to synchronize the seismic signals with direct observations and the use of a seismometer that was not capable ~~of recording such high frequencies~~ to record the high-frequency energy of the generated seismic waves might explain why the analytic relationships were not confirmed by this experiment.

In this study we propose a new field experiment of controlled releases of single blocks to investigate the ~~relations~~ relationships between block properties and dynamics, and the ~~associated seismic signal features~~ features of the seismic signals generated by impacts with the slope. We deployed several short-period and broadband seismic stations to record the high-frequency seismic signal generated at each impact ~~on soft-rock substrate~~. The trajectory of each block is reconstructed with video cameras ~~that were synchronized with the seismometers~~. The seismic signal processing allowed us ~~to retrieve~~ inferring the amplitude of the seismic signal at the source, corrected from propagation effects, and the ~~energy of the seismic radiation generated~~ seismic energy radiated by the impacts. We then compare the features of the seismic signal of each impact to the dynamics and the properties of the released block.

25 **2 The ~~Rieux-Bourdoux~~ Rieux-Bourdoux experiment**

The ~~Rieux-Bourdoux~~ Rieux-Bourdoux controlled releases experiment ~~main focus is~~ focus was to study the seismic signal of single-block rockfalls on unconsolidated soft-rock, which ~~are~~ is highly attenuating for seismic waves. The ~~Rieux-Bourdoux~~ Rieux-Bourdoux is a torrent located in the ~~french~~ French Alps, approximately 4 km north of the town of Barcelonnette (France). The slopes surrounding the torrent consist ~~mainly~~ of Callovo-Oxfordian black-marls and are representative of the ~~slopes~~ slope morphology of marly facies observed in south-east France. Due to the high erosion susceptibility of black marls ~~and marls in general~~, numerous steep gullies have formed on these slopes.

We conducted ~~our releases experiment~~ the releases within one of these gullies (Figure 1a and b). The advantage of launching the ~~block~~ blocks in a gully is that for every block the traveled path is roughly ~~similar~~ the same. Moreover, the steepness of

the gullies that developed in black-marls allows the block to rapidly reach a high velocity. The travel path had a length of approximately 200 meters and slope angles ranging from ~ 45 degrees on the upper part of the slope to ~ 20 degrees on the terminal debris cone. 28 blocks with mass ranging from 76 to 472 kg were manually launched.

Two video camera were deployed (Sony alpha7 - 25 frame per seconds) allowing to record the movement of the blocks. They were deployed at the feet base of the gully, close to the torrent. Ground-controlled Ground-control points were marked for visual recognition on the videos and their 3D coordinates taken via GNSS were measured by Global Navigation Satellite System (GNSS). A reference Digital Elevation Model (DEM) at a spatial resolution of 0.5 m was built from terrestrial LIDAR acquisitions (Figure 1c). The time of the cameras was set to be synchronous with the seismic sensor time (GPS). The seismic monitoring device network was composed of 1 broadband seismometer (CMG40T - sampling frequency 100 Hz) located north of the gully, and an antenna of 4 short-period seismometers (one 3 component and three with 1 vertical component - sampling frequency 1000 Hz) located south of the gully (Figure 1c).

3 Methods

3.1 Trajectory reconstruction and dynamic parameters estimation

To reconstruct the trajectory, the impacts of each block were manually picked on the frames of the videos. Thanks to the control points, the frames of the videos can be projected on the DEM. Hence, once an impact is identified on the frame, the position of the pixel is reported on the DEM, which gives the true position of the impact in space. This processing is repeated for the two cameras, which gives an estimate of the uncertainties on the determination of the position and the time of the impact. The velocity just before impact is derived from the block trajectory and the duration of block flight before impact. The kinetic energy was computed as:

$$E_k = \frac{1}{2} m V^2, \quad (1)$$

with m the mass of the block and V the velocity before impact. We also determined the potential energy lost during the block flight before impact from the difference of altitude of the block between two impacts, inferred from the reconstructed trajectory, as:

$$E_p = mg(h_{t_1} - h_{t_2}), \quad (2)$$

with g the gravitational acceleration, and h_{t_1} and h_{t_2} the altitudes of the block at the impacts that occurred at the two successive times t_1 and t_2 . Unfortunately, the resolution of the cameras and the complex dynamics of the blocks during the first seconds of propagation did not allow us to identify clearly the impacts on the upper part of the slope. However the trajectory trajectories of the blocks on the lower part of the slope is well constrained, with an average uncertainty on the inferred velocity of the blocks before impacts of 0.95 m s^{-1} for velocities with values comprised between 6 m s^{-1} and 17 m s^{-1} .

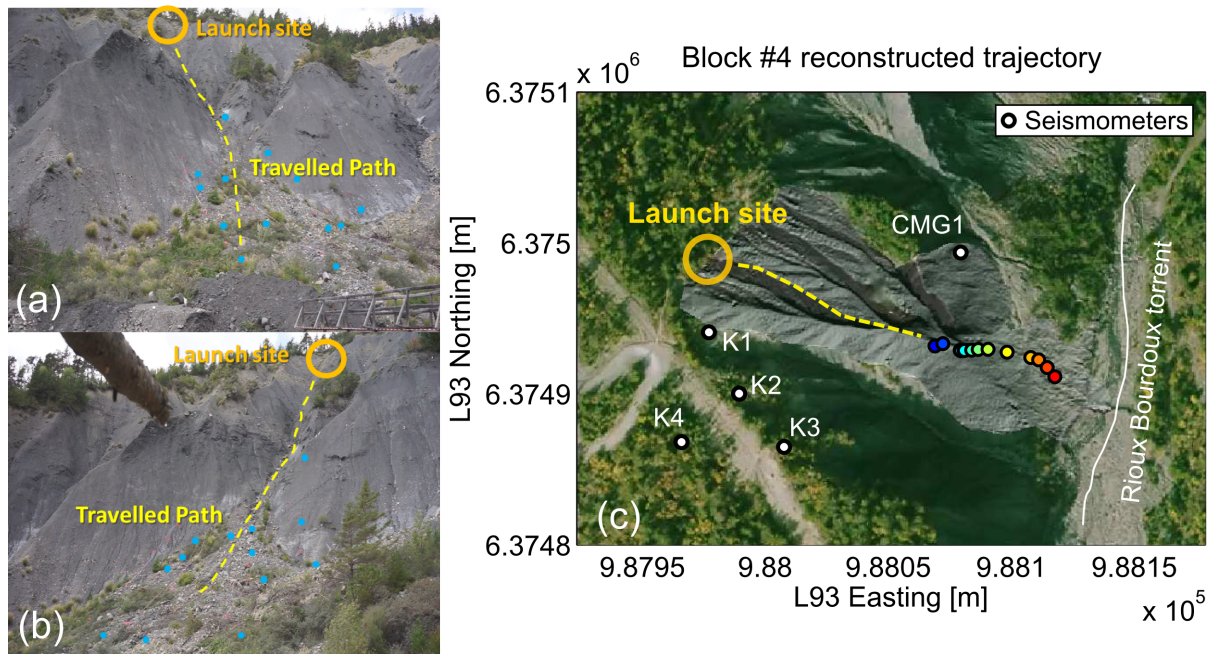


Figure 1. View from a) the first and b) the second video cameras deployed at the bottom of the slope. The ground control points are indicated by blue points. c) Trajectory reconstruction for block 4 on the DEM, built from LIDAR acquisition, superimposed on an orthophoto of the Rioux-Bourdoux-Rioux-Bourdoux slopes. Each point indicates the position of an impact and the color gradient represents the chronology of these impacts (blue for the first impact and red for the last one). K2 is a three-component short-period seismometer and K1, K3 and K3 are vertical-only seismometers. CMG1 is a broad-band seismometer.

3.2 Seismic signal processing

Seismic waves are Several authors have shown that the seismic waves generated by gravitational instabilities are dominated by surface waves (e.g. Deparis et al., 2008; Hibert et al., 2011; Dammeier et al., 2011; Levy et al., 2015). These high-frequency seismic surface waves are subjected to strong propagation effects, especially in a highly attenuating medium such as black marls. Figure 2 shows the seismic signals recorded for the launch of the block number 4. The attenuation is visible when comparing peaks in the seismic signal recorded at the station located on the upper part of the slope (Figure 2a) to the ones recorded at the station on the lower part of the slope (Figure 2c), for the same time. The amplitude of the peaks is clearly dependent of-on the distance between the impact and the seismic station. Moreover, Figure 2b shows the attenuation of the highest frequency with the distance of the source to the seismic station. To compare seismic signal features to the dynamic

parameter of the rockfall, we have to correct these attenuation effects. Aki and Chouet (1975) proposed a simple attenuation law giving the amplitude $A(r)$ of a seismic surface wave recorded at a distance r as:

$$A(r) = \frac{1}{\sqrt{r}} A_0 \times e^{-Br}. \quad (3)$$

If the distance between the station and the source is known, the computation of the amplitude at the source A_0 is straightforward. However we have to determine the frequency dependent parameter B that accounts for the anelastic attenuation of seismic waves. If we consider r_i the distance between the source and station i and r_j the distance to station j ~~we have, the~~ apparent anelastic attenuation parameter B_{ij} is then:

$$B_{ij} = \frac{\log(A(r_i)\sqrt{r_i}) - \log(A(r_j)\sqrt{r_j})}{\sqrt{r_j} - \sqrt{r_i}}. \quad (4)$$

By combining Eq. (3) and Eq. (4), we can compute the amplitude at the source A_0 for each pair of stations. This value is then averaged over all the pairs of stations, and the standard deviation gives an estimate of the uncertainty.

~~The other~~ Another quantity that we want to compare to the dynamics of the block is the radiated seismic energy. The ~~seismic~~ energy of a seismic surface wave can be computed as (Crampin, 1965):

$$E_s = \int_{t_i}^{t_f} 2\pi r \rho D h c u_{env}(t)^2 e^{Br} dt, \quad (5)$$

with :

$$u_{env}(t) = \sqrt{u(t)^2 + Ht(u(t))^2}, \quad (6)$$

where Ht is the Hilbert transform of the seismic signal $u(t)$ used to compute the envelope $u_{env}(t)$, t_i and t_f the times of the beginning and the end of the seismic signal respectively, h the thickness and ρD the density of the layer through which the generated surface waves propagate, and c their phase velocity. The average velocity of surface waves in black-marls formations observed in the area of the Rioux Bourdoux torrent is approximately 300 m/s (Hibert et al., 2012; Gance et al., 2012), which, for seismic signal with central frequencies around 20 Hz (Figure 2) $f = 20 \text{ Hz}$ as observed on Figure 2, gives a propagation depth h , computed as $h = c/f$, of $\sim 15 \text{ m}$. The density ρD of dry black-marls is approximately 1450 kg m^{-3} (Maquaire et al., 2003).

Before computing the amplitude at the source and the energy of the seismic signals generated by impacts, we first selected the seismic signals with the following criteria: ~~i) we excluded from our analysis.~~ We excluded the seismic signals generated when i) sliding of the blocks occurred; ~~ii) when,~~ ii) the blocks stopped mid-slope and iii) more generally when the signal-to-noise ratio was too weak on the seismic stations to perform the computation of the ~~parameter B .~~ B apparent anelastic attenuation

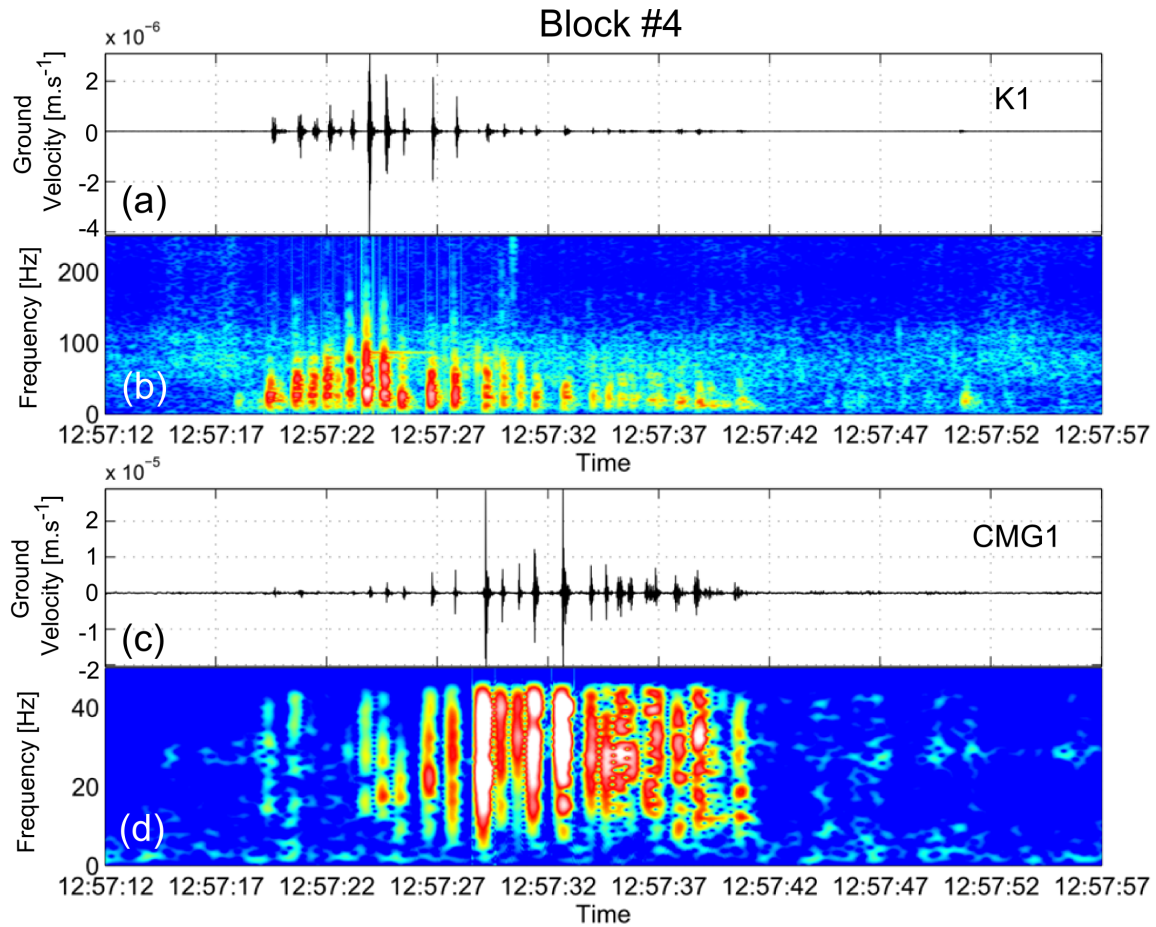


Figure 2. a) Signal recorded at the short-period station located on the upper part of the slope and b) corresponding spectrogram, generated by block number 4 (mass of 209 kg). c) Signal recorded at the broadband station located on the lower part of the slope and d) corresponding spectrogram, generated by block 4.

parameter B_{ij} . B_{ij} is dependent on the frequency of the seismic waves. Therefore the seismic signals were band-pass filtered between 1 and 50 Hz. This frequency band is chosen because most of the seismic wave energy is not attenuated in this band within the span of the seismic network (Figure 2b and d). For each seismic record selected, we manually picked the peaks corresponding to the impacts on each station. This processing results in a data set of 37 impact seismic signals, coming from 9

5 out of the 28 launches.

4 Results

4.1 Correlation between dynamic parameters and seismic signal features

From the reconstructed trajectories we inferred the velocity, the momentum and the kinetic energy of the block before each impact (Eq. 1), and the potential energy lost during the block trajectory before impact (Eq. 2). The velocities exhibit a low variability, with values ranging from 6 m s^{-1} to 17 m s^{-1} (Figure 3). We did not find significant correlation between the mass and the impact velocity.

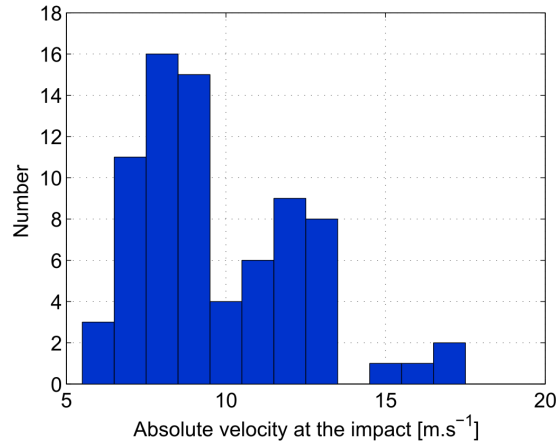


Figure 3. Histogram of the observed absolute velocities before impact.

The seismic signal processing ~~allowed us to infer the yielded the maximum~~ amplitude at the source ~~and the seismic energy of the seismic signal of the impacts~~ $A0_{max}$ and the radiated seismic energy E_s at each impact. The average uncertainty on the computation of the maximum amplitude $A0_{max}$, inferred from the standard deviation, and expressed as a percentage of the computed values (i.e. $A0_{max} \pm x\%A0_{max}$), ranges from 7% to 129%, and is 58% in average. Regarding the computation of the ~~seismic energy~~ radiated seismic energy E_s , the uncertainty, estimated following the same approach, ranges from 55% to 152% of the computed values, and is 86% in average.

We investigated the possible ~~correlation~~ correlations between: 1) the maximum amplitude at the source $A0_{max}$ of the seismic signal and the absolute momentum $|p|$ before the impact; 2) the radiated seismic energy E_s and the potential energy lost E_p ; 3) the ~~seismic energy~~ radiated seismic energy E_s and the kinetic energy E_k before impact; and 4) the radiated seismic energy E_s and the mass m of the blocks. ~~We computed for the four cases regression lines of the data set to investigate possible correlation between the selected quantities. As all the point distribution appears to be following a linear trend (Figure 4), we computed the best regression line following equation:-~~

$$Y = \alpha X + \beta,$$

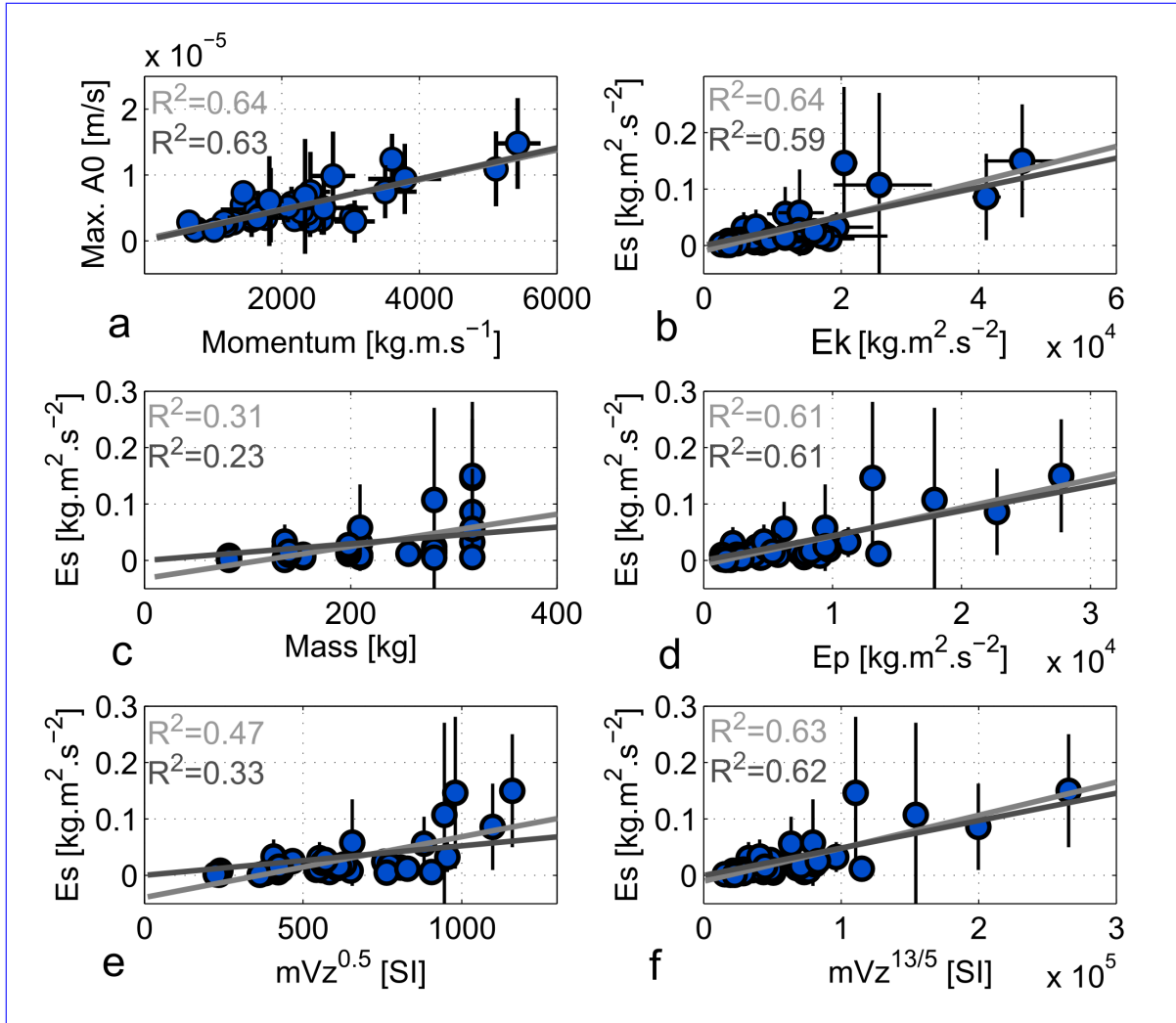


Figure 4. a) Decimal-logarithm-Maximum of the maximum-of-the-amplitude $A_{0,max}$, corrected from attenuation, as a function of the decimal-logarithm-of-the-average momentum $|p|$ of the block before the impact. b) Decimal-logarithm-of-the-Radiated seismic energy E_s of the seismic signal generated at the impact as a function of: b) the decimal-logarithm-of-the-kinetic energy before the impact E_k ; c) Decimal-logarithm of the seismic energy E_s as a function of the decimal-logarithm-of-the-masses m of the blocks; d) Decimal-logarithm of the seismic energy E_s of the seismic signal generated at the impact as a function of the decimal-logarithm-of-the-potential energy lost E_p ; e) Decimal-logarithm of the seismic energy E_s as a function of the decimal-logarithm-of-the-parameter $mVz^{0.5}$; f) Decimal-logarithm of the seismic energy E_s as a function of the decimal-logarithm-of-the-parameter $mVz^{13/5}$. Errors bars resulting from the computation of the momentum, the kinetic energy and the amplitude at the source are indicated by black lines. For each pair of parameters the light-gray line corresponds to the best regression line computed for a linear relationship and the dark-gray one to the best regression line computed for a proportional relationship.

The analysis based on the Hertz's theory of impact conducted by Farin et al. (2015) yielded the parameter $mV_z^{13/5}$, with m the mass of the block and V_z the vertical velocity before impact, that should in theory scale with the radiated seismic energy E_s of the seismic signal generated at each impact. However, when investigating this relationship for real single-block rockfalls, they did not found a significant correlation with this parameter. The best correlation they found was with the parameter α and β of the regression line given in Table 1 for each case, in the logarithmic and linear scales: $mV_z^{0.5}$. We also investigated these two cases with our data set. We computed for each pair of parameters the Spearman rank correlation coefficient ρ and the corresponding p - values (Table 1) (Spearman, 1904) as we assume that the parameters should scale following monotonic laws.

The best correlation is found coefficient ρ has a value of 0.70 for the pair of parameters E_s and E_k . Slightly lower correlation coefficient values are observed between the maximum amplitude $A0_{max}$ and the absolute momentum $|p|$ ($\rho = 0.67$) and the radiated seismic energy E_s and the kinetic energy E_k , with R^2 values of 0.64. There is no significant correlation between the mass m and the potential energy E_p ($\rho = 0.68$). The correlation coefficient between the radiated seismic energy E_s as suggested by the low R^2 values of 0.31 and 0.39 of the regression lines. Overall the R^2 values do not exceed 0.64, which is caused by and the high variability of the data. This high variability comes from the high uncertainties on the computation of the seismic attenuation parameters which in return impact the computed values of best empiric parameter $mV_z^{0.5}$ found by Farin et al. (2015) is poorer ($\rho = 0.62$) than the one observed between the radiated seismic energy and the parameter $mV_z^{13/5}$ they derived from the Hertz theory of impact ($\rho = 0.69$). Finally, our results show that there is no correlation between the maximum amplitude $A0_{max}$ and the radiated seismic energy E_s , as shown by the large error bars on Figure 4 ($\rho = 0.44$) and between the radiated seismic energy E_s and the mass of the blocks m ($\rho = 0.51$). We also investigated other correlations between dynamic parameters and seismic signal features, with the vertical momentum or the vertical kinetic energy for example, but we were unable to improve on the correlations found with the modulus of the dynamic quantities.

The analysis based on the Hertz's theory of impact conducted by Farin et al. (2015) yielded the parameter $mV_z^{13/5}$. To characterize the relationships between the parameters that are correlated, we computed the regression lines that best fit the data (Figure 4 and Table 1). According to the theoretical analysis conducted by Farin et al. (2015), the dynamic parameters should scale proportionally with m the mass of the block and V_z the vertical velocity before impact, that should in theory scale with the seismic energy features. However several studies have shown that linear relationships allow a better fitting of the data gathered from the observation of natural events (e.g. Deparis et al., 2008; Dammeier et al., 2011; Hibert et al., 2011). We computed the regression coefficients of the best fitting lines for the two types of relationships and assessed the quality of the fitting by computing the coefficients of determination R^2 .

Overall the R^2 coefficient values do not exceed 0.64 (Table 1). This is caused by a high scattering of the data which comes from the high uncertainties on the computation of the seismic attenuation parameters and hence on the values of $A0_{max}$ and E_s generated at each impact. However, when investigating this relationship for real single-block rockfalls, they did not found a significant correlation with this parameter, as shown by the large error bars on Figure 4. The best correlation they found was with the parameter $mV_z^{0.5}$. We investigated the two cases with our data set. We found that the parameter derived from Hertz's theory of impact yields a better correlation than the optimal parameter found in Farin et al. (2015), with R^2 values of 0.57–0.63

and 0.47–0.49 respectively (Figure ??e, f, and Table 1) coefficients are yielded by the linear regression between the maximum amplitude $A0_{max}$ and the momentum $|p|$, and the radiated seismic energy E_s and the kinetic energy E_k ($R^2 = 0.64$ for both cases). For the couple of parameters E_s/E_p and $E_s/mV_z^{13/5}$, R^2 coefficients are slightly lower, with values of 0.61 and 0.63 respectively. The regression of each pair of parameters by proportional relationships gives lower values for the coefficient R^2 . However the β coefficients of the best linear regressions are close to 0. We assume that linear regressions allow to better accommodate for the scattering of the data than proportional regressions, and that β coefficients are not physically significant.

4.2 Retrieving block properties and dynamics from the seismic signal

We have shown that correlations exist between ~~some several~~ dynamics quantities and features of the seismic signal generated at each impact. In this section we investigate if these relationships can provide accurate estimates of the mass and the velocity of the blocks, directly from the features of the seismic ~~signal generated by signals generated by the~~ impacts.

~~By combining Eq. (??) Our results show that the maximum amplitude and the seismic energy are not correlated (Table 1). Hence we can combine the linear relationships inferred~~ for the maximum amplitude and the momentum, and for the radiated seismic energy and the kinetic energy, with the coefficients α and β ~~computed in the linear scale, we yielded by the linear regressions.~~ We can express the mass m_i as a function of $A0_{max}$ and E_s as:

$$m_i = \frac{5.9 \times 10^{11} (A0_{max} - 2.50 \times 10^{-7})^2}{(E_s + 0.01)}. \quad (7)$$

Using Eq. (7), we computed m_i for each impact of each block for which we were able to compute $A0_{max}$ and E_s , and compared the average estimates of m_i to the measured mass m_r of each block (Table 2). Overall, the inferred masses m_i are close to the real masses m_r of the block. However, the uncertainty on the inferred values is high, especially for ~~block blocks~~ for which we have a few number of exploitable impacts and therefore few estimates of $A0_{max}$ and E_s . This may also come from the uncertainties related to the computation of the seismic quantities.

We can also estimate the velocity of the block before each impact using ~~Eq. ?? with the correlation parameters the linear regression and the corresponding coefficients~~ found between the maximum amplitude $A0_{max}$ and the maximum momentum p , or between the seismic energy E_s and the kinetic energy E_k , and with the masses inferred with Eq. 7. We choose to use the ~~linear~~ relationship between the amplitude and the momentum because the uncertainties ~~on the determination of the associated~~ with determining the amplitude at the source are lower than ~~the one on the those associated with the radiated~~ seismic energy. The inferred velocity V_i can be computed as:

$$V_i = \frac{A0_{max} - 2.50 \times 10^{-7}}{2.26 \times 10^{-9} m_i}. \quad (8)$$

Figure 5a shows the distribution of the absolute difference between the velocities inferred V_i and the velocities V_r derived from the trajectory reconstruction. The values of the difference are comprised between 0.1 and 13.7 ms^{-1} , with a median value of 2.4 ms^{-1} . We also computed the ratio of the ~~velocities-velocity absolute~~ $|V_i - V_r|$ difference over the ~~velocities-velocity~~

derived from the trajectory reconstruction V_r (Figure 5b). The majority of the values of the ratio falls below 0.5 (i.e. the difference is less than 50% of the value of the velocity derived from the trajectory reconstruction), and the median ratio is 0.2 (i.e. 20% of the value of the velocity derived from the trajectory reconstruction).

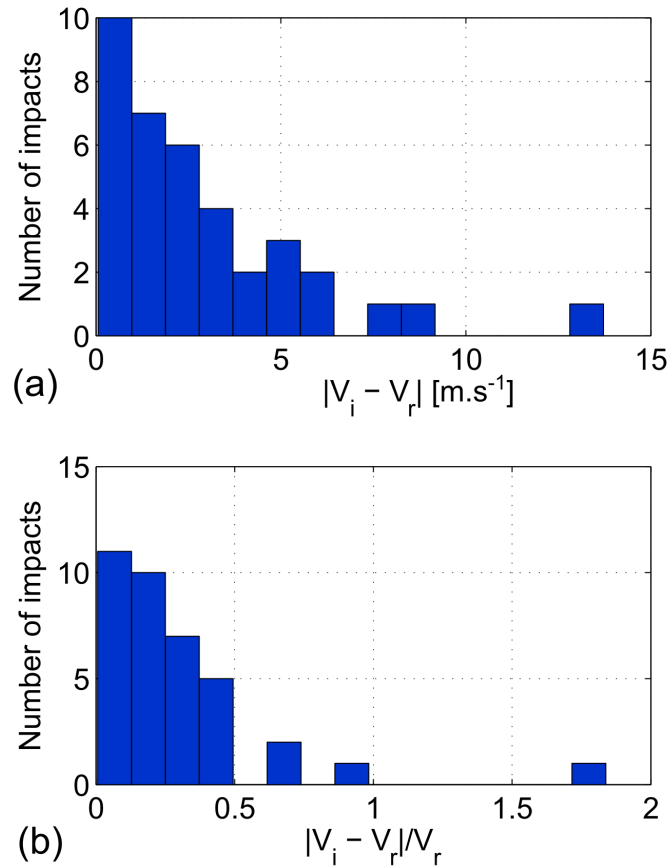


Figure 5. a) Histogram showing the distribution of the difference between the velocity before impact V_i inferred using Eq. [??-7](#) and Eq. [5-8](#) and the velocity V_r estimated ~~thanks-to-from~~ the video cameras; b) Same as a) but normalized by the value of the velocity V_r estimated via the video cameras.

5 Discussion and conclusion

- The Rioux-Bourdoux experiment of controlled single-block rockfalls ~~yields important results for understanding produced~~ [important results to better understand](#) the links between the dynamics of rockfalls and the seismic signal associated. Our results suggest that ~~linear-sealing correlations~~ [exist](#) between the seismic signal features and the dynamic quantities of single-block

rockfalls. We observed that the maximum amplitude of the seismic signal generated at each impact and the momentum (product of the mass and the velocity) of the blocks are correlated. Our results also suggest that the energy of the seismic radiation released at each impact scales linearly with the potential energy lost and the kinetic energy. Despite large uncertainties, mainly caused by the simple seismic attenuation model used, the scaling laws found permit to infer realistic values of the masses and the velocities before impact of the blocks from the amplitude and the energy of the seismic signal generated.

We found that the relationship derived from the Hertz's theory of impact proposed by Farin et al. (2015) that links the radiated seismic energy of the signal generated to the parameter $mV_z^{13/5}$ is verified with our data. ~~This scaling was not confirmed for controlled single-block rockfalls in their study. They assume this was caused by the changing properties of the soil along the path and the low sampling frequency of the seismometer used that prevented to measure the totality of the seismic energy released at each impact. In our study the instruments we deployed permitted to record most of the energy generated at impacts. This underlines the importance of choosing adequate seismometers, capable of recording the whole seismic energy generated at the impacts, for future studies.~~

~~The~~ However the scaling between the seismic energy and the parameter $mV_z^{13/5}$ did not yield a significantly better quantitative correlation than the one observed between the radiated seismic energy and the kinetic energy, or between the amplitude at the source and the momentum of the block before impact (best R^2 of 0.63, 0.64 and 0.64 $\rho = 0.69, 0.70$ and 0.67 respectively). This confirms the combined role of the mass and the velocity before impacts of the block in the generation of seismic waves, but does not allow us to identify a unique dynamic parameter that would control the seismic signal features. Further analytic analytical and theoretical developments are needed to understand the physical processes that explain these correlations, and ultimately what are the physical parameters that control the characteristics of the seismic signal generated.

~~These relationships~~ An issue that arose from studies on the link between the seismic signals and the dynamics of mass movements is about the energy transfer and more specifically the ratio $R_{s/p}$ between the radiated seismic energy and the potential energy lost. Deparis et al. (2008) found for 10 rockfalls that occurred in the French Alps that this $R_{s/p}$ ratio is comprised between 10^{-5} and 10^{-4} . Vilajosana et al. (2008) have found a $R_{s/p}$ ratio of 10^{-3} for an artificially triggered rockfalls in the Montserrat massif (Spain). In volcanic contexts, Hibert et al. (2011) and Levy et al. (2015) have observed $R_{s/p}$ ratios ranging from 10^{-5} to 10^{-3} . In this study, we found a $R_{s/p}$ ratio between the radiated seismic energy and the potential energy lost of approximately 10^{-6} (Table 1). Interestingly a ratio of the same order is observed between the radiated seismic energy and the kinetic energy. The value of the $R_{s/p}$ ratio is lower than those observed in other contexts. We assume that this might be explained by the nature of the substrate as in our case the rockfalls propagated on unconsolidated soft-rocks, which may absorbed more potential energy (by deformation for example) than consolidated igneous (Hibert et al., 2011; Levy et al., 2015) or metamorphic rocks (Deparis et al., 2008; Vilajosana et al., 2008). Investigating this assumption on the role of the substrate on energy transfer by replicating the experiment of controlled releases of single blocks in other contexts constitutes one of the perspectives of this work.

The relationships found open the possibility to estimate directly the mass and the dynamic parameters of single-block rockfalls from the generated seismic signal. However, we identified several limitations that have to be addressed before considering an operational application of seismology to quantify rockfall properties. First, our results show that better attenuation models

are needed to reduce the uncertainties on the computation of the seismic signal features. ~~Second, the coefficients of the scaling laws we found between the different quantities may be controlled by the geological context. More similar studies performed in other contexts are needed to assess their potential impact on these relationships.~~ ~~Third~~ This could be achieved by deploying denser seismic networks for example. ~~Second~~, the range of the mass of the blocks used in our experiment spans only one order of magnitude. The behavior of the relationships we found has to be investigated for a larger range of volumes. This again underlines the relevance and the necessity of reproducing similar studies in new contexts.

Finally, our results give a new insight on the processes that generate high-frequency seismic signals associated with rock-falls, landslides, rock-avalanches, and granular flows in general. We show that the maximum amplitude of the seismic signal generated by the impact of a single particle is proportional to its ~~momentum~~ mass and velocity. In a granular flow, a very large quantity of particles ~~interacts~~ interact with themselves and with the substrate at a given time. The ~~source of the seismic signal generated at this given time might therefore be the sum of the impulses imparted by the particles to the ground.~~ The magnitude of these impulses ~~may~~ imparted on the Earth by each particle might be controlled by the ~~momentum~~ mass and the velocity of the particles within the flow according to the ~~scaling law we found~~ correlations we observed. The issue is now to understand what controls the ~~momentum~~ dynamics of the particles within the flow and how their complex interactions influence the generation of seismic waves. This should be more thoroughly investigated, using numerical granular flow models for example, and is probably the key to model the high-frequency seismic signal associated with gravitational instabilities in the future.

6 Code and Data availability

The codes and the data used in this study are accessible upon request by contacting C. Hibert (hibert@unistra.fr).

Author contributions. C. Hibert, J.-P. Malet, F. Bourrier and F. Provost participated in the acquisition and the processing of the seismic and kinematic data. F. Berger, P. Tardif and E. Mermin helped to design and perform the Rioux Bourdoux experiment, and for the acquisition of the video and the reconstruction of the trajectories of the blocks. P. Bornemann performed the Lidar survey and the processing of the data that allow reconstructing the DEM of the gully into which blocks have been launched.

Competing interests. The authors declare that they have no conflict of interest.

Acknowledgements. We are very grateful toward Anne Mangeney for helpful discussions and insightful suggestions, and to Georges Guiter (RTM) for organizing the practical details and the security of the experimental launch site. This work was carried with the support of the French National Research Agency (ANR) through the projects HYDROSLIDE 'Hydrogeophysical Monitoring of Clayey Landslides' and SAMCO 'Adaptation de la Société aux Risques Gravitaires en Montagne dans un Contexte de Changement Global' and of the Open Partial Agreement Major Hazards of Council of Europe through the project 'Development of cost-effective ground-based and remote monitoring systems for detecting landslide initiation'. The ~~seismometers used in this experiment belong~~ data were acquired using instruments belonging to the French national pool of portable ~~seismic instruments SISMOB-RESIF~~ seismic stations RESIF-SISMOB (CNRS-INSU).

References

- Aki, K. and Chouet, B.: Origin of coda waves: source, attenuation, and scattering effects, *Journal of geophysical research*, 80, 3322–3342, 1975.
- Allstadt, K.: Extracting source characteristics and dynamics of the August 2010 Mount Meager landslide from broadband seismograms, *Journal of Geophysical Research*, 118, 1472–1490, doi:10.1002/jgrf.20110, 2013.
- 5 Amitrano, D., Grasso, J. R., and Senfaute, G.: Seismic precursory patterns before a cliff collapse and critical point phenomena, *Geophysical Research Letters*, 32, 2005.
- Burjánek, J., Moore, J. R., Molina, F. X. Y., and Fäh, D.: Instrumental evidence of normal mode rock slope vibration, *Geophysical Journal International*, 188, 559–569, 2012.
- 10 Burtin, A., Hovius, N., Milodowski, D. T., Chen, Y.-G., Wu, Y.-M., Lin, C.-W., Chen, H., Emberson, R., and Leu, P.-L.: Continuous catchment-scale monitoring of geomorphic processes with a 2-D seismological array, *Journal of Geophysical Research: Earth Surface*, 118, 1956–1974, 2013.
- Chen, C.-H., Chao, W.-A., Wu, Y.-M., Zhao, L., Chen, Y.-G., Ho, W.-Y., Lin, T.-L., Kuo, K.-H., and Chang, J.-M.: A seismological study of landquakes using a real-time broad-band seismic network, *Geophysical Journal International*, 194, 885–898, 2013.
- 15 Clouard, V., Athanase, J.-E., and Aubaud, C.: Physical characteristics and triggering mechanisms of the 2009–2010 landslide crisis at Montagne Pelée volcano, Martinique: implication for erosional processes and debris-flow hazards, *Bulletin de la Société Géologique de France*, 184, 155–164, 2013.
- Crampin, S.: Higher modes of seismic surface waves: Second Rayleigh mode energy, *Journal of Geophysical Research*, 70, 5135–5143, 1965.
- 20 Dammeier, F., Moore, J. R., Haslinger, F., and Loew, S.: Characterization of alpine rockslides using statistical analysis of seismic signals, *Journal of Geophysical Research*, 116, F04024, doi:10.1029/2011JF002037, 2011.
- Dammeier, F., Moore, J. R., Hammer, C., Haslinger, F., and Loew, S.: Automatic detection of alpine rockslides in continuous seismic data using Hidden Markov Models, *Journal of Geophysical Research: Earth Surface*, 121, 351–371, 2016.
- Deparis, J., Jongmans, D., Cotton, F., Baillet, L., Thouvenot, F., and Hantz, D.: Analysis of rock-fall and rock-fall avalanche seismograms in the French Alps, *Bulletin of the Seismological Society of America*, 98, 1781–1796, doi:10.1785/0120070082, 2008.
- 25 Ekström, G. and Stark, C. P.: Simple scaling of catastrophic landslide dynamics, *Science*, 339, 1416–1419, doi:10.1126/science.1232887, 2013.
- Farin, M., Mangeney, A., Toussaint, R., Rosny, J. d., Shapiro, N., Dewez, T., Hibert, C., Mathon, C., Sedan, O., and Berger, F.: Characterization of rockfalls from seismic signal: Insights from laboratory experiments, *Journal of Geophysical Research: Solid Earth*, 120, 7102–7137, doi:10.1002/2015JB012331, 2015JB012331, 2015.
- 30 Favreau, P., Mangeney, A., Lucas, A., Crosta, G., and Bouchut, F.: Numerical modeling of landquakes, *Geophysical Research Letters*, 37, L15305, doi:10.1029/2010GL043512, 2010.
- Galea, P., D’Amico, S., and Farrugia, D.: Dynamic characteristics of an active coastal spreading area using ambient noise measurements—Anchor Bay, Malta, *Geophysical Journal International*, 199, 1166–1175, 2014.
- 35 Gance, J., Grandjean, G., Samyn, K., and Malet, J.-P.: Quasi-Newton inversion of seismic first arrivals using source finite bandwidth assumption: Application to subsurface characterization of landslides, *Journal of Applied Geophysics*, 87, 94–106, 2012.

- Helmstetter, A. and Garambois, S.: Seismic monitoring of Séchilienne rockslide (French Alps): Analysis of seismic signals and their correlation with rainfalls, *Journal of Geophysical Research*, 115, F03 016, doi:10.1029/2009JF001532, 2010.
- Hertz, H.: Über die Berührung fester elastischer Körper., *Journal für die reine und angewandte Mathematik*, 92, 156–171, 1882.
- Hibert, C., Mangeney, A., Grandjean, G., and Shapiro, N. M.: Slope instabilities in Dolomieu crater, Réunion Island: From seismic signals to rockfall characteristics, *Journal of Geophysical Research*, 116, F04 032, doi:10.1029/2011JF002038, 2011.
- Hibert, C., Grandjean, G., Bitri, A., Travelletti, J., and Malet, J.-P.: Characterizing landslides through geophysical data fusion: Example of the La Valette landslide (France), *Engineering Geology*, 128, 23–29, 2012.
- Hibert, C., Ekström, G., and Stark, C. P.: Dynamics of the Bingham Canyon Mine landslides from seismic signal analysis, *Geophysical Research Letters*, 41, 4535–4541, doi:10.1002/2014GL060592, 2014a.
- 10 Hibert, C., Mangeney, A., Grandjean, G., Baillard, C., Rivet, D., Shapiro, N. M., Satriano, C., Maggi, A., Boissier, P., Ferrazzini, V., and Crawford, W.: Automated identification, location, and volume estimation of rockfalls at Piton de la Fournaise volcano, *Journal of Geophysical Research: Earth Surface*, 119, 1082–1105, doi:10.1002/2013JF002970, <http://dx.doi.org/10.1002/2013JF002970>, 2014b.
- Hibert, C., Stark, C. P., and Ekström, G.: Seismology of the Oso-Steelhead landslide, *Nat. Hazards Earth Syst. Sci. Discuss.*, pp. 7309–7327, 2014c.
- 15 Hibert, C., Ekström, G., and Stark, C. P.: The relationship between bulk-mass momentum and short-period seismic radiation in catastrophic landslides, Submitted to *Journal of Geophysical Research: Earth Surface*, 2017.
- Levy, C., Jongmans, D., and Baillet, L.: Analysis of seismic signals recorded on a prone-to-fall rock column (Vercors massif, French Alps), *Geophysical Journal International*, 186, 296–310, 2011.
- Levy, C., Mangeney, A., Bonilla, F., Hibert, C., Calder, E. S., and Smith, P. J.: Friction weakening in granular flows deduced from seismic records at the Soufrière Hills Volcano, Montserrat, *Journal of Geophysical Research: Solid Earth*, 120, 7536–7557, 2015.
- 20 Maquaire, O., Malet, J.-P., Remaitre, A., Locat, J., Klotz, S., and Guillon, J.: Instability conditions of marly hillslopes: towards landsliding or gullying? The case of the Barcelonnette Basin, South East France, *Engineering Geology*, 70, 109–130, 2003.
- Moretti, L., Mangeney, A., Capdeville, Y., Stutzmann, E., Huggel, C., Schneider, D., and Bouchut, F.: Numerical modeling of the Mount Steller landslide flow history and of the generated long period seismic waves, *Geophysical Research Letters*, 39, L16 402, doi:10.1029/2012GL052511, 2012.
- 25 Norris, R. D.: Seismicity of rockfalls and avalanches at three Cascade Range volcanoes: Implications for seismic detection of hazardous mass movements, *Bulletin of the Seismological Society of America*, 84, 1925–1939, 1994.
- Panzer, F., D’Amico, S., Lotteri, A., Galea, P., and Lombardo, G.: Seismic site response of unstable steep slope using noise measurements: the case study of Xemxija bay area, Malta, *Natural Hazards and Earth System Sciences*, 12, 3421, 2012.
- 30 Schneider, D., Bartelt, P., Caplan-Auerbach, J., Christen, M., Huggel, C., and McArde, B. W.: Insights into rock-ice avalanche dynamics by combined analysis of seismic recordings and a numerical avalanche model, *Journal of Geophysical Research*, 115, F04 026, doi:10.1029/2010JF001734, 2010.
- Spearman, C.: The proof and measurement of association between two things, *The American journal of psychology*, 15, 72–101, 1904.
- Tripolitsiotis, A., Daskalakis, A., Mertikas, S., Hristopoulos, D., Agioutantis, Z., and Partsinevelos, P.: Detection of small-scale rockfall incidents using their seismic signature, in: *Third International Conference on Remote Sensing and Geoinformation of the Environment*, pp. 953 519–953 519, International Society for Optics and Photonics, 2015.
- 35

Vilajosana, I., Suriñach, E., Abellán, A., Khazaradze, G., Garcia, D., and Llosa, J.: Rockfall induced seismic signals: case study in Montserrat, Catalonia, Natural Hazards and Earth System Sciences, 8, 805–812, doi:10.5194/nhess-8-805-2008, http://www.nat-hazards-earth-syst-sci.net/8/805/2008/nhess-8-805-2008.html, 2008.

5 Yamada, M., Matsushi, Y., Chigira, M., and Mori, J.: Seismic recordings of landslides caused by Typhoon Talas (2011), Japan, Geophysical Research Letters, 39, L13 301, doi:10.1029/2012GL052174, 2012.

Yamada, M., Kumagai, H., Matsushi, Y., and Matsuzawa, T.: Dynamic landslide processes revealed by broadband seismic records, Geophysical Research Letters, 40, 2998–3002, doi:10.1002/grl.50437, 2013.

Zimmer, V. L. and Sitar, N.: Detection and location of rock falls using seismic and infrasound sensors, Engineering Geology, 193, 49–60, 2015.

<u>Parameters (X, Y)</u>	<u>Spearman correlation</u>		<u>Proportional</u>			<u>linear</u>		
	<u>ρ</u>	<u>p-values</u>	<u>α</u>	<u>β</u>	<u>R^2</u>	<u>α</u>	<u>β</u>	<u>R^2</u>
<u>$A0_{max} = \alpha p + \beta$</u>	<u>0.67</u>	<u>$1.12 \cdot 10^{-7}$</u>	<u>$2.35 \cdot 10^{-9}$</u>	<u>0</u>	<u>0.63</u>	<u>$2.26 \cdot 10^{-9}$</u>	<u>$2.50 \cdot 10^{-7}$</u>	<u>0.64</u>
<u>$E_s = \alpha E_p + \beta$</u>	<u>0.68</u>	<u>$6.75 \cdot 10^{-6}$</u>	<u>$4.40 \cdot 10^{-6}$</u>	<u>0</u>	<u>0.61</u>	<u>$5.04 \cdot 10^{-6}$</u>	<u>-0.01</u>	<u>0.61</u>
<u>$E_s = \alpha E_k + \beta$</u>	<u>0.70</u>	<u>$3.01 \cdot 10^{-6}$</u>	<u>$2.59 \cdot 10^{-6}$</u>	<u>0</u>	<u>0.59</u>	<u>$3.09 \cdot 10^{-6}$</u>	<u>-0.01</u>	<u>0.64</u>
<u>$E_s = \alpha m + \beta$</u>	<u>0.51</u>	<u>$1.3 \cdot 10^{-3}$</u>	<u>$1.48 \cdot 10^{-4}$</u>	<u>0</u>	<u>0.23</u>	<u>$2.85 \cdot 10^{-4}$</u>	<u>-0.03</u>	<u>0.31</u>
<u>$E_s = \alpha m V_z^{13/5} + \beta$</u>	<u>0.69</u>	<u>$4.16 \cdot 10^{-6}$</u>	<u>$4.86 \cdot 10^{-7}$</u>	<u>0</u>	<u>0.62</u>	<u>$5.85 \cdot 10^{-7}$</u>	<u>-0.01</u>	<u>0.63</u>
<u>$E_s = \alpha m V_z^{0.5} + \beta$</u>	<u>0.62</u>	<u>$7.63 \cdot 10^{-5}$</u>	<u>$5.24 \cdot 10^{-5}$</u>	<u>0</u>	<u>0.33</u>	<u>$1.07 \cdot 10^{-4}$</u>	<u>-0.04</u>	<u>0.47</u>
<u>$A0_{max} = \alpha E_s + \beta$</u>	<u>0.44</u>	<u>$8.2 \cdot 10^{-3}$</u>	<u>-</u>	<u>-</u>	<u>-</u>	<u>-</u>	<u>-</u>	<u>-</u>

Table 1. Spearman correlation coefficients, coefficients of the regression lines for proportional and linear relationships and corresponding coefficient of determination R^2 .

<u>Block #</u>	<u>m_r [kg]</u>	<u>m_i [kg]</u>	<u>std.</u>	<u>Nbr. impacts</u>
9	281	198	56	5
1	318	334	71	6
4	209	208	115	7
35	82	84	68	3
33	256	97	-	1
22	154	171	146	3
20	198	211	39	6
17	136	181	118	4
13	140	270	162	2

Table 2. Comparison between the real mass m_r of the blocks and the average inferred masses m_i computed with Eq. 7.

10 ~~Parameters (X, Y) α β R^2 α β R^2 $A0_{max} = \alpha p + \beta$ 0.84 -8.12 0.58 $2.26 \cdot 10^{-9}$ $2.50 \cdot 10^{-7}$ 0.64 $E_s = \alpha E_p + \beta$ -1.17 -6.05 0.54 $5.04 \cdot 10^{-6}$ -0.01 0.61 $E_s = \alpha E_k + \beta$ 1.38 -7.34 0.60 $3.09 \cdot 10^{-6}$ -0.01 0.64 $E_s = \alpha m + \beta$ 1.9 -6.23 0.39 $2.85 \cdot 10^{-4}$ -0.03 0.31 $E_s = \alpha m V_z^{13/5} + \beta$ 1.43 -8.60 0.57 $5.85 \cdot 10^{-7}$ -0.01 0.63 $E_s = \alpha m V_z^{0.5} + \beta$ 2.02 -7.42 0.49 $1.07 \cdot 10^{-4}$ -0.04 0.47~~

Coefficients of the regression lines